# Heterogeneous atmospheric aerosol chemistry: laboratory studies of chemistry on water droplets

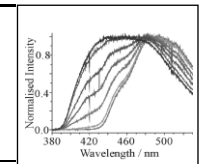


**Jonathan P. Reid* and Robert M. Sayer**

*School of Chemical Sciences, University of Birmingham, Edgbaston, Birmingham, UK B15 2TT. E-mail: j.reid@bham.ac.uk*

***Received 1st October 2002***
***First published as an Advance Article on the web 23rd January 2003***

**Heterogeneous chemical reactions on aerosol particles play a pivotal role in atmospheric chemistry. In this review, the fundamental concepts underlying the chemical dynamics of liquid aerosol droplets are discussed, with particular emphasis on the properties of the aqueous–air interface and the reaction mechanisms of key chemical processes. Recent laboratory studies of heterogeneous chemistry on aqueous aerosol particles are reviewed, with techniques that probe the gas phase, liquid phase and the interface directly, discussed in turn.**

## 1 Introduction

Although the Earth's atmosphere is predominantly gaseous, the discovery of the Ozone Hole and the observation of acid rain confirmed the role of aerosols in mediating important atmospheric chemical reactions. Condensed phase reactions in the bulk of an aerosol particle and heterogeneous reactions on the particle surface can provide alternative reaction mechanisms to those that can occur in the homogeneous gas phase. A chemical reaction between neutral closed shell molecules may have a prohibitively large activation barrier as a gas phase reaction. However, in the condensed phase, the solvation of ionic intermediates can provide a reaction pathway with a lower activation energy permitting the reaction to occur through an ionic reaction mechanism. For aerosol chemistry to play a significant role in influencing the chemical balance of the atmosphere, the diffusion of reagents in the gas phase to the particle surface, their subsequent heterogeneous reaction and release of the products from the particle surface into the gas phase, must compete efficiently with the rate of the corresponding homogeneous gas phase reaction.

Acid rain results from the atmospheric oxidation of the oxides of sulfur and nitrogen to sulfuric acid and nitric acid, respectively, with atmospheric aerosols playing a significant role in this process.[1] Anthropogenic pollution, principally from fossil fuel combustion, is the dominant source of atmospheric $SO_2$, with natural sources only accounting for ~10% of the atmospheric concentration. Although $SO_2$ can be oxidised in the homogeneous gas phase, $SO_2$ removal from the atmosphere can occur more rapidly than the oxidation process. That the oxidation proceeds more rapidly under conditions of high humidity or when condensed water is available, suggests that oxidation may be mediated by aqueous atmospheric aerosol particles. The reaction proceeds initially by the formation of ionic intermediates in the condensed phase.

$$SO_{2(ads)} + H_2O \Leftrightarrow H^+_{(aq)} + HSO_3^-{}_{(aq)} \quad (1a)$$

$$HSO_3^-{}_{(aq)} \Leftrightarrow H^+_{(aq)} + SO_3^{\,2-}{}_{(aq)} \quad (1b)$$

The $HSO_3^-$ intermediate is oxidised by dissolved ozone ($O_3$) or hydrogen peroxide ($H_2O_2$).

$$HSO_3^-{}_{(aq)} + OH^- + O_3 \rightarrow H_2O + SO_4^{\,2-}{}_{(aq)} + O_2 \quad (1c)$$

Other oxidants in urban environments, which can participate by more complex chain processes involving radical-ion intermediates, include the radicals OH and $HO_2$.

Atmospheric aerosols are dispersions of either solid particles or liquid droplets within the atmospheric gas phase. Examples of solid aerosols include smoke and dust, while clouds, fogs and mists are liquid aerosols. Particles range in diameter from 10 nm to 100 μm, with typical tropospheric concentrations of 10–1000 particles in a volume of 1 $cm^3$ for particles smaller than 1 μm.[1] Larger particles have lower concentrations, with typically less than 1 particle $cm^{-3}$. Particles can be multiphase and multicomponent, with the particle composition determined by the primary origin and by chemical processing and aging of the

*Dr Jonathan Reid completed his DPhil at the University of Oxford in 1997 before moving to JILA, University of Colorado, to work as a Postdoctoral Research Associate. As a Lecturer in Physical Chemistry at the University of Birmingham from 2000, he is now developing optical laser-based techniques to probe the chemistry of aerosol droplets. He was awarded the 2001 Harrison Medal by the Royal Society of Chemistry.*

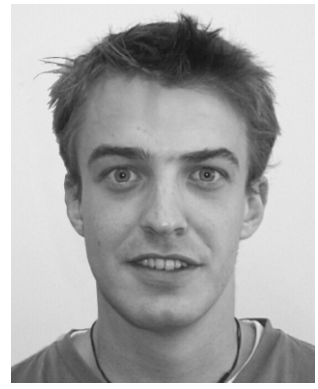

*Dr Rob Sayer completed his undergraduate degree in chemistry at the University of York followed by an MRes degree in Earth and Atmospheric Sciences at the University of Reading. He returned to York to read a PhD in heterogeneous atmospheric chemistry. He is currently a Postdoctoral Research Associate at the University of Birmingham studying aerosol science.*

 DOI: 10.1039/b204463n

particle during its atmospheric lifetime. The primary source of particles can be natural, such as soil and mineral dust, sea salt and biological debris, or anthropogenic, with origins such as combustion and industrial dust. Owing to the turbulent nature of the troposphere, aerosols from different sources readily mix, leading to multicomponent aerosols incorporating inorganic ions through to large organic species, such as terpenes.[1] This can yield aerosols of varying hygroscopic character and varying aqueous content.

With water ubiquitous in the atmosphere, all aerosol particles contain an aqueous component. A generic aerosol particle may consist of solid aggregates of solid salts in equilibrium with aqueous dissolved species. Surrounding these aggregates is the aqueous medium, which acts to hold the aggregates together. The water content of the aerosol is dependent on the relative humidity (RH), which is defined as the ratio of the water vapour density to the saturation water vapour density, usually expressed as a percentage. Thus, a fully saturated atmosphere has a RH value of 100% and a dry (desert) atmosphere will have a value close to 0%. If the RH of the atmosphere increases, at a RH known as the deliquescence point, a solid anhydrous particle will begin to grow as water condenses onto the particle surface, as illustrated in Fig. 1. Ammonium sulfate has a deliquescence point of 75% RH, at which point it absorbs water forming a hydrated salt solution.

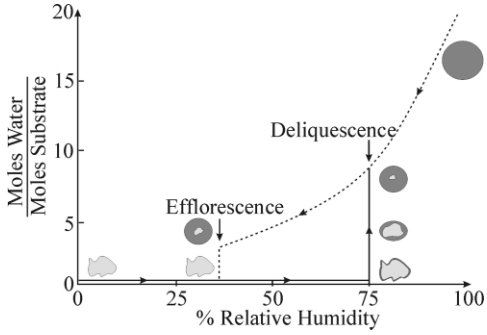


**Fig. 1** The deliquescence and efflorescence points of a soluble inorganic salt.

For solid multicomponent aerosols, it is important not only to know the salt composition but also the solubility of each component. This knowledge will ultimately determine the partitioning within the aerosol particle between the solid, hydrated or liquid phase. At different degrees of hydration, the identity of the dominant dissolved ion can vary, leading to a significant change in droplet pH. An aqueous solution of ammonium sulfate (2.5 M) has a pH of 6.6, significantly different from a sodium chloride solution, which has a pH of 7.3. Thus, ammonium sulfate and sodium chloride aerosol droplets will present a different degree of acidity to any adsorbing gas. In addition, the identity of the dominant dissolved ion can influence reactions occurring on the aerosol droplet. The rate of the oxidation of $SO_2$ in cloud droplets is determined by the relative water content and droplet pH. These properties are dependent on the growth in water content of the droplet, with smaller droplets often showing enhanced condensation rates and, hence, different compositions to larger droplets.[1] Thus, cloud droplets of different sizes can have different oxidative abilities for converting $SO_2$ to acid sulfates.

If the atmospheric RH falls, an aqueous droplet containing dissolved inorganic salts will remain a solution to lower RHs than the deliquescence point. A solid nucleus forms at the efflorescence point, and this is controlled by the crystallisation kinetics of the inorganic salt within the solution phase. Energy barriers to crystallisation cause salt droplets to supersaturate, forming highly concentrated metastable solutions before efflorescence occurs. If a solid nucleus exists within the solution phase, the relative humidity of efflorescence can be dramatically altered. Heterogeneous nucleation on the pre-existing nucleus reduces the crystallisation energy barrier allowing rapid formation of the solid salt.

With the atmospheric context of the origin and importance of aqueous aerosol droplets now established, this review article will aim to define the fundamental factors which influence chemical reactions on aqueous aerosol droplets. Initially, the nature of the liquid water–air interface will be explored, with this controlling the interaction between the gas and condensed phases. The elementary processes that lead to the progress of chemical reactions in aqueous aerosol droplets will then be reviewed, along with a molecular view of the chemical dynamics that occur at the liquid interface. The unique reactivity of the liquid interface of aerosol droplets will be discussed. Recent developments in our understanding of the chemical reactions of aqueous aerosol droplets from fundamental laboratory studies will then be reviewed.

## 2 A molecular view of dynamics at the liquid–gas interface

A molecular view of liquid interfaces is extremely complex, primarily because the interfacial region cannot be considered in isolation. The molecular dynamics at the interface are inextricably linked to processes occurring in the gas and liquid phases surrounding the interface. We will discuss the unique properties of liquid interfaces, before reviewing a description of the multiphase kinetics of aerosols. A molecular mechanism that leads to the transport of molecules between the bulk gas phase and condensed aerosol phase, through the interfacial region, will then be discussed.

### 2.1 The liquid interface

Liquid interfaces are extremely dynamic with the diffusion of molecules to and from the interface leading to complete surface reconstruction on a timescale of microseconds.[2] Approximately three million monolayers per second are transferred between the liquid and gas phase for a water surface at 0 °C with a vapour pressure of ~5 Torr.[3] The interfacial region is intermediate in character between the bulk gas and liquid phases, with the transition between the two bulk phase molecular concentrations occurring over a distance of few molecular layers, as illustrated in Fig. 2. Such heterogeneous character is also directly reflected in the surface tension of the interface. The surface tension is a measure of the difference in the Gibbs free energy between molecules in the bulk of the droplet and those at the interface.[2] Water molecules at the interface experience fewer hydrogen bonds than molecules within the isotropic liquid phase due to the asymmetry of the interface. Partial solvation at the interface is energetically less favourable than full solvation within the bulk, and this leads to droplets adopting a spherical shape. The surface tension is defined as the energy required to increase the surface area by 1 square unit through transportation of molecules from the bulk to the interface. Water has a surface tension of 72 mJ $cm^{-2}$, which is relatively large for liquid surfaces, reflecting the interactions occurring at a molecular level and the strong hydrogen bonding in bulk water.

The laser technique Second Harmonic Generation (SHG) has been employed to probe the structure of interfacial water. SHG is a non-linear optical technique in which photons with a frequency of $\omega$ are converted to photons of frequency $2\omega$ by interaction with a non-centrosymmetric environment. The SHG signal at $2\omega$ results only from the asymmetric interface, and is not generated by an isotropic bulk phase, providing a direct probe of the interfacial region. The SHG studies indicate that the

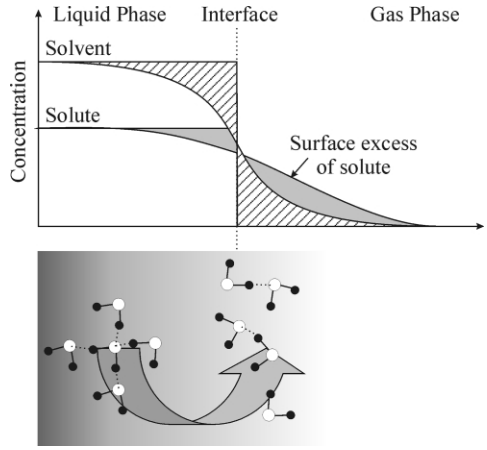


**Fig. 2** The transition between the bulk liquid and gas phases occurs in the interfacial region over a distance of a few molecular layers. The surface tension (surface free energy) reflects the energy required to bring molecules from the bulk liquid phase to the interface, increasing the surface area by 1 unit.

average dipole moment vector of the water lies nearly parallel to the interface, although the hydrogen atoms are on average located slightly below the surface.[4] Similar studies by Shen[5] used a technique called Sum Frequency Generation (SFG) in which a visible and an infrared (IR) photon are combined by the non-linear optical process of SFG at the asymmetric interface. The frequency of the IR photon is tuned, providing a resonantly enhanced SFG signal when it is matched in frequency to the vibrational frequency of a molecule in the interfacial region. This not only provides a direct probe of the interface, but also a chemically specific probe, enabling the proportions of free and hydrogen bonded OH groups near the interface to be determined. These studies indicated that ~20% of interfacial water molecules have dangling OH bonds (~$2 \times 10^{14}$ molecules $cm^{-3}$), pointing away from the surface, which are free from hydrogen bonding. This percentage of free OH bonds changes with solution pH.[6] The SHG studies have also indicated that the concentration of $H^+$ at the interface can be as much as two orders of magnitude lower than in the bulk phase.

Solute molecules may preferentially adsorb to the interface rather than undergoing full solvation in the bulk liquid phase. Full solvation may lead to such disruption of the hydrogen-bonding network of water molecules that the energetically most favourable position for the solute is adsorption at the interface. This permits recreation of the hydrogen-bonding network in the bulk phase. Solutes that preferentially adopt a surface configuration are known as surfactants. Surfactant molecules that have a hydrophilic head group and a hydrophobic tail, adopt an orientation at an aqueous interface in which the hydrophilic head group is directed toward the aqueous interface and the hydrophobic tail is directed away. This results in an enhanced solute concentration at the interface over that in the bulk phase, referred to as a surface excess concentration. Surface tension measurements of aqueous solutions of numerous alcohols and organic acids show that the binding of the organic molecule to the water interface becomes progressively more favourable over bulk solvation with increasing hydrocarbon chain length.[7] The estimated surface coverage of ~$10^{14}$ molecules $cm^{-2}$, is approximately 10% of the underlying density of water molecules, or ~50% of those with free hydrogen bonds.

If the surfactant species is charged, a surface potential results leading to a non-uniform distribution of charged ions near the interface. Counter-ions preferentially diffuse towards the liquid interface to balance the surface charge, while ions of the same polarity as the surfactant species diffuse away from the interface, leading to the formation of an electric double layer. This double layer may extend for tens of nanometers from the interface, depending on the surface potential and the concentration of ions in the bulk. Increasing the ionic strength of the aqueous phase leads to a balancing of the surface charge over a shorter distance into the bulk.

Sulfuric acid and nitric acid are the most abundant atmospheric acids and it is appropriate to consider their influence on the interfacial water structure. SFG studies suggest that at a sulfuric acid mole fraction of 0.1, the number of dangling free OH bonds from the interface is greatly reduced.[3,8] Water is bound as sulfate hydrates at the surface, and thus the surface is depleted of free water. At the lower concentrations studied for aqueous nitric acid solutions, with mole fractions as low as 0.005, an electric double layer is formed. The large polarisable anions approach the interface and the less polarisable cations lag at greater depths.[9] At higher nitric acid concentrations, ionic complexes approach the interface, disrupting the hydrogen bonding network and perturbing the top water layers. Surface tension measurements support this view with a decrease in surface tension with increase in nitric acid concentration. At high concentrations, contact ion pairs form, such as $H_3O^+NO_3^-$, leading to a collapse of the electric double layer and a complete disruption of the hydrogen bonding network at the surface. [9]

The passage of molecules between the gas and liquid phases through the interface is dependent on the unique properties of the interfacial region. In the same way as the surface tension is related to a Gibbs free energy difference between solvent molecules in the bulk liquid and at the interface, we must consider the change in Gibbs free energy accompanying transfer of a solute molecule from the gas phase to the surface adsorbed state, followed by diffusion into the liquid and solvation.

### 2.2 Mass accommodation at the liquid interface

The growth or evaporation of a liquid droplet as molecules are transported to or away from the interface in the gas phase leads to an evolution of droplet temperature, composition and mass.[10] The coupled differential equations which describe these changing properties must also account for the change in temperature and partial pressure in the gas phase. Although the physical and chemical dynamics of an aerosol droplet are most accurately described by such a set of coupled differential equations, decoupling the processes occurring in the gas and bulk liquid and at the interface enables a simple physical picture of the multiphase kinetics to be gained.

One approach that decouples the multiphase processes leads to an analogy with the resistances in an electrical circuit.[11,12] The flux of a trace gas into the bulk of a liquid droplet is determined by the combined rate of a series of fundamental processes, each of which can be assigned a resistance. Gas-phase transport of the trace molecule to the liquid interface is followed by accommodation at the liquid interface and subsequent transport into the bulk liquid away from the interfacial region, as illustrated in Fig. 3a. Each of these processes, and the limitations they impose on the flux of molecules between the bulk phases through the interface, will now be described for a soluble non-reactive trace gas.

The flux of molecules in the gas phase to the liquid surface can be calculated from the gas-kinetic flux, $J_{gk}$, which assumes that the collision frequency of gas phase molecules with the surface can be determined from the ambient pressure surrounding the droplet. However, as gas phase molecules are accommodated at the interface, the gas-phase composition near the interface becomes depleted, and diffusion towards the droplet occurs. If transfer across the interface is facile, the rate of gas phase diffusion can limit the flux into the aerosol droplet. This presents a significant resistance to transfer into the droplet, or conversely a low conductance, $\Gamma_{gd}$.

On striking the interface, the molecule may enter the condensed phase or desorb. The probability that a molecule will

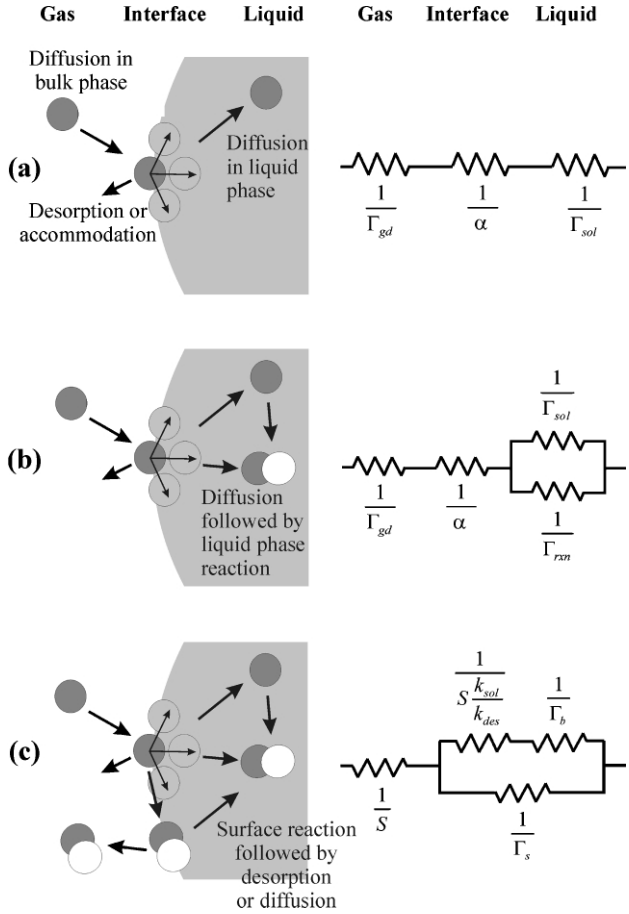


**Fig. 3** The resistance model for uptake for the three scenarios discussed in the text: (a) non-reactive uptake, (b) non-reactive uptake with bulk phase reaction, (c) reactive uptake with bulk phase reaction.

enter the condensed phase is referred to as the mass accommodation coefficient, $\alpha$.

$$\alpha = \frac{\text{Number of molecules adsorbed by the interface}}{\text{Number of molecules striking the interface}} \quad (2)$$

The flux of molecules into the droplet, $J$, can be expressed as $J_{gk}\alpha$, or in terms of the number density of molecules in the gas phase, $n_g$ (molecules cm$^{-3}$), and the average speed of the trace gas molecules, $c$, as

$$J = \frac{n_g c \alpha}{4} \quad (3)$$

This determines the maximum flux/rate of transfer of molecules across the interface. The surface coverage is then determined by the total flux to and from the interface, taking into account both the gas and the condensed phases.

Accommodation is followed by diffusion into the bulk phase. This can critically limit the flux of molecules into the droplet: the interface may rapidly become saturated with the trace gas if the probability of accommodation is large and if there are no gas-diffusion limitations, preventing further accommodation. Over time, the partitioning of the trace gas between the gas and liquid phase will approach an equilibrium state determined by Henry's law, *i.e.* the solubility of the trace gas in the condensed phase. As the partitioning approaches this equilibrium state, the transfer conductance, $\Gamma_{sol}$, from the interface into the bulk phase decreases. At equilibrium, the flux into the condensed phase is equal to the flux of desorbing molecules from the interface.

The limitations imposed on the accommodated flux by gas-phase diffusion to and liquid phase diffusion away from the interface act to limit the flux into the droplet under most conditions. This is accounted for by replacing the mass accommodation coefficient by an uptake coefficient, $\gamma$,

$$J = \gamma J_{gk} \quad (4)$$

where

$$\frac{1}{\gamma} = \frac{1}{\alpha} + \frac{1}{\Gamma_{gd}} + \frac{1}{\Gamma_{sol}}. \quad (5)$$

This treatment assumes that the accommodated molecule does not undergo reaction.

### 2.3 The mechanism of uptake

The mass accommodation of a molecule at the liquid interface initially involves transient adsorption at the surface, followed by transfer into the bulk phase, which competes with desorption back into the gas phase. This is illustrated in Fig. 4. The first

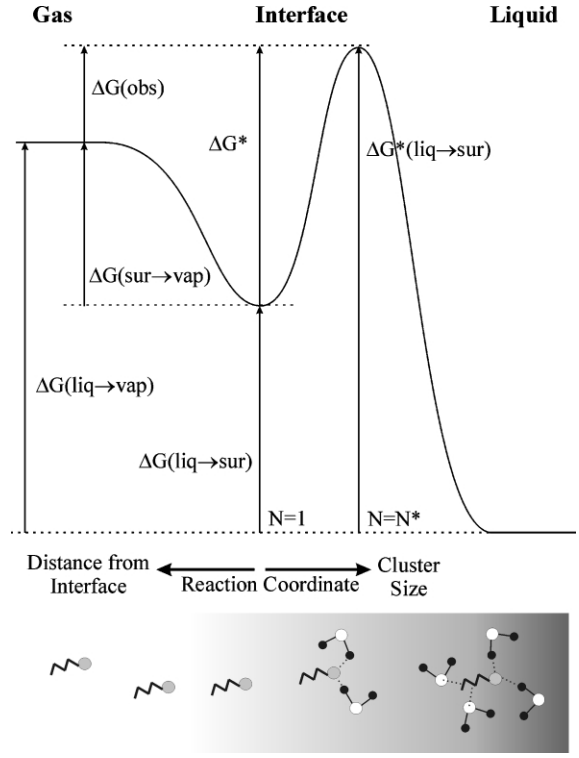


**Fig. 4** The Gibbs free energy profile for accommodation at a liquid–air interface. Following thermal accommodation at the surface, mass accommodation is governed by the formation of a critical cluster and progress over the Gibbs free energy barrier. [Reprinted with permission from *J. Phys. Chem.* 1996, **31**, 13016. Copyright 1996 American Chemical Society.]

step involves energy transfer from the adsorbing molecule to the liquid surface, leading to thermal accommodation. Although the probability of this occurring is frequently assumed to be unity, the energy transfer process is dependent on the mass of the gas and surface molecules and the angle and kinetic energy of the collision. Thermal accommodation is least efficient for light mass gas molecules colliding with heavy surface groups, and for collisions occurring at high impact energies (equivalently high temperatures).[11]

Significant insights into the mechanism of accommodation can be acquired from the temperature dependence of the mass accommodation coefficient. An inverse temperature dependence is indicative of the uptake of a species which is soluble in water. From the temperature dependence of $\alpha$, the Gibbs free energy change between the isolated gas-phase molecules and the transition state lying between the gas and liquid states ($\Delta G_{obs}$, defined in Fig. 4) can be estimated. The associated values of $\Delta H_{obs}$ and $\Delta S_{obs}$ can thus be calculated. For species soluble in water, $\Delta H_{obs}$ and $\Delta S_{obs}$ are correlated and are

independent of the size/shape of the molecule.[13] Unexpectedly, $\Delta H_{obs}$ is inversely correlated with the hydrogen bonding ability of the solute.

The mechanism of transfer of molecules from the interface into the bulk involves the progression from a transient adsorbed species into a fully solvated solute. At a microscopic level, the change in entropy of the accommodated molecule can be described as the loss in free volume as the solute molecule enters the denser liquid phase, and the change in ordering of the solvent molecules as the solute becomes fully solvated within the bulk liquid. This occurs over a short distance in the interfacial region. However, the enthalpy change occurs over a longer distance range. Interactions between solute and solvent form as the molecule approaches the interface, reaching the full solvation enthalpy within the bulk phase.[14]

Ballistic encounters of gas molecules with the interface do not possess sufficient kinetic energy to displace solvent molecules for direct incorporation of the solute within the bulk phase. An initial mechanism for accommodation proposed that incorporation into the bulk phase occurs by the formation of a microscopic cavity of appropriate size for the solute molecule to occupy. The formation of such a cavity is expected to be endothermic ($\Delta H_{cav} > 0$ kJ mol$^{-1}$), with the magnitude of the enthalpy dependent on the size of the cavity that must form to accommodate the solute. Although formation of solvent–solute interactions is exothermic, this model does not support the experimental trend that $\Delta H_{obs}$ is always exothermic. It also suggests that the solutes that hydrogen-bond to the solvent water most strongly should exhibit the most exothermic values of $\Delta H_{obs}$. This is the reverse of the observed trend.

An alternative mechanism for mass accommodation has been proposed that considers the interfacial region as a narrow region of dense gas in which nucleation is continually occurring.[13] The dynamic nature of the liquid interface suggests that such nucleation can readily occur, leading to the partial solvation of the adsorbed solute. A critical cluster must form around the adsorbed solute before transport into the bulk phase is energetically allowed. Evaporation from the liquid surface occurs by the surfacing of a critical cluster from within the bulk phase, followed by the lessening of partial solvation until the solute can escape the interfacial region. This critical cluster can be described as a surface analogue of a solvation shell, with the critical cluster regarded as local density fluctuations in the solvent around the solute in the interfacial region.[7] $\Delta H_{obs}$ and $\Delta S_{obs}$ are related to the energetics of forming the critical cluster, which contains $N^*$ monomers composed of $N^*$-1 solvent molecules and the solute.

Once the critical cluster is formed, there is no barrier to transport of the critical cluster from the interface to the bulk phase. This is illustrated in Fig. 4. The energetic barrier to accommodation in the bulk is entropic in origin. The formation of the critical cluster is favoured enthalpically through partial solvation of the solute, but is entropically unfavourable, primarily because of the exchange of the solute from the gas to liquid phase. The Gibbs free energy for formation of a cluster at the surface increases to a maximum with increase in cluster size, $N$, before diminishing. Clusters that are smaller than the critical cluster size, which contains $N^*$ monomers, evaporate and mass accommodation does not result. Clusters larger than the critical size can grow further and can become incorporated within the bulk phase. The ability of the solute molecule to act as a nucleating centre for forming the critical cluster determines how facile it is for the solute to be accommodated within the water phase. The orientation of the solute molecule with respect to the bulk liquid and the depth of penetration through the interfacial region determine the number of water molecules required for formation of the critical cluster. At the lower densities encountered on the gas side of the interfacial region, the critical cluster size required for transport into the bulk phase is larger than at deeper penetration depths.

Theoretical studies of the uptake of ethanol at a water interface have questioned the existence of a barrier to accommodation, predicting a mass accommodation coefficient of unity.[7] However, the critical cluster model supports the experimental observations of $\alpha < 1$ and the correlation between $\Delta H_{obs}$ and $\Delta S_{obs}$. The larger the critical cluster that the solute must form before progress along the minimum energy pathway to bulk solvation can occur, the larger the exothermicity of the observed enthalpy for accommodation, $\Delta H_{obs}$. Consequently, the larger the ordering of solvent molecules around the solute and the more negative $\Delta S_{obs}$.

### 2.4 Heterogeneous and condensed phase reactions

In addition to the mass accommodation and diffusion processes already discussed, chemical reaction can occur at the interface of the droplet, or following diffusion of reactants into the bulk of the droplet. The former is most accurately termed a heterogeneous reaction, while the latter is properly described by bulk phase chemistry. The chemical conversion of an accommodated species may act to offset the saturation of the condensed phase, permitting continual uptake of the gas phase reactant beyond the level predicted by Henry's law. This illustrates that bulk phase solvation and chemical reaction are directly coupled. In most experiments, one of these two processes is designed to dominate the other. Eqn. 5 can be refined to account for the rate of bulk phase chemical reaction, $\Gamma_{rxn}$, as illustrated in Fig. 3b.

$$\frac{1}{\gamma} = \frac{1}{\alpha} + \frac{1}{\Gamma_{gd}} + \frac{1}{\Gamma_{sol} + \Gamma_{rxn}} \quad (6)$$

If the solubility of the trace gas is low, the conductance $\Gamma_{sol}$ is small, and if the reaction rate is fast, then $\Gamma_{rxn}$ is large, and eqn. 6 can be written as

$$\frac{1}{\gamma} = \frac{1}{\alpha} + \frac{1}{\Gamma_{gd}} + \frac{1}{\Gamma_{rxn}}. \quad (7)$$

Following reaction, the product molecules may remain solvated within the bulk, lie at the interface, or may evaporate into the gas phase.

Heterogeneous reactions are thought to occur directly in the interfacial region for the uptake of some trace gases, such as $SO_2$, $NH_3$ and the reaction of $ClONO_2$ with HCl.[15] All of the gases that show enhanced surface reactivity are able to form stable ionic complexes at the interface by hydrolysis. For example, $SO_2$ can form $HSO_3^-$ $H^+$ and $NH_3$ can form $NH_4^+$ $OH^-$.[11] This competes with mass accommodation and reaction in the bulk liquid phase. Following the initial thermal accommodation of the gas phase species at the interface, now referred to as having a sticking probability $S$, hydrolysis of the surface species occurs at a faster rate than solvation by formation of the critical cluster and diffusion into the bulk. This is accounted for in the refined resistance diagram, illustrated in Fig. 3c. The uptake coefficient is defined in terms of the sticking probability, followed by competition between surface reaction, $\Gamma_s$, and bulk dissolution followed by reaction. The latter can be broken down into two sequential processes: (1) competition between desorption and solvation of the thermally accommodated molecules at the interface and (2) reaction in the bulk phase, $\Gamma_b$. This can be expressed by the sequence of processes:[16]

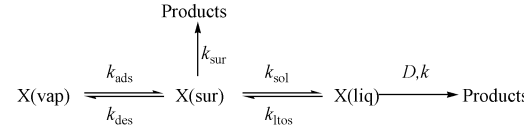


$k_{ads}$, $k_{des}$, $k_{sol}$, $k_{ltos}$, $k_{sur}$, $k$ are the rate constants for adsorption, desorption, solvation, transfer of the solute from the liquid to the

surface, surface reaction and reaction in the bulk phase, respectively. The progress from X(sur) to X(liq) represents the transfer from the surface adsorbed state, over the barrier into the bulk liquid, shown in Fig. 4, and does not make any assumptions about the rate of this process.

The uptake coefficient is now expressed as the reaction probability, the fraction of collisions of a gas-phase molecule with the surface that lead to reaction.[16]

$$\frac{1}{\gamma} = \frac{1}{S} + \frac{1}{\dfrac{1}{\dfrac{1}{\Gamma_b} + \dfrac{1}{S\dfrac{k_{sol}}{k_{des}}}} + \Gamma_s} \quad (8)$$

This formulation is derived from considering the flux of X between the gas phase, interface and bulk. First, the net flux from the gas phase to the interface is equated to the difference in flux between absorption and desorption. Secondly, the difference in net fluxes from the gas to interface (from processes $k_{ads}$ and $k_{des}$) and bulk to interface (from processes $k_{sol}$ and $k_{ltos}$) is equated to the surface reactive flux, under steady state conditions. Finally, the net flux into the liquid (from processes $k_{sol}$ and $k_{ltos}$) is equated to the diffusion flux into the liquid from Fick's law. This formulation may not, however, be applicable if the surface coverage of the adsorbing molecule becomes high, and a significant proportion of the surface sites are occupied.

The competition between reactive loss at the surface and within the bulk phase is now inherently included. Hanson[16] notes that the mass accommodation parameter may not be a meaningful parameter when considering a reactive uptake process which is dominant at the interface. The fraction of molecules lost to reaction at the surface will have a direct impact on the fraction of molecules undergoing accommodation within the bulk phase. As the rate of surface reactive loss increases, the rate of reactive loss in the bulk phase must similarly decrease due to a decreased flux of reactant molecules into the bulk. A redefinition of $\alpha$ as the fraction of molecules incorporated in the liquid to the total number available for incorporation may be a more appropriate definition.

Experimentally, surface and bulk reactions can be differentiated by examining the dependence of the uptake coefficient on the concentration of a second reactant within the droplet. If a linear dependence is observed, the reactive uptake is best considered as progressing with a heterogeneous surface reaction. The enhanced rate of a surface reaction may reflect the unique properties of the surface, such as increased reagent concentrations at the interface due to surface excess or electric double layer formation. For example, it has been suggested that an enhanced oxidation rate of $Cl^-$ in sea-salt aerosol could be attributed to a greater coverage of the air–solution interface by large polarizable anions than by small non-polarisable cations.[6] The degree of surface exposure of each ion present in solution could influence interfacial reactivity towards gas phase reactants. Alternatively, the enhanced surface rate may be due to the existence of a rapid reaction pathway that occurs before the molecule has diffused more than a few molecular diameters into the bulk phase.

## 3 Laboratory studies of chemical reactions on droplets

Heterogeneous reactions on aerosol droplets can be probed by examining the change in the composition of the gas phase or the condensed phase, or by targeting the interfacial region directly. Each of these three approaches yields complementary information on the multiphase chemical dynamics and kinetics that are occurring. Recent developments in examining heterogeneous reactions of atmospheric importance by these three approaches will now be described; this discussion will be limited to experimental work published during the last five years. A comprehensive review of earlier work can be found in reference 12.

### 3.1 Probing the gas phase

Experimental methods that probe the depletion of the gas phase species as accommodation onto a liquid surface proceeds have yielded many important insights into heterogeneous chemistry. The dominant techniques for uptake measurements on liquids have been the droplet train technique, the wetted-wall flow tube technique, and the entrained aerosol flow tube. These techniques have been described in detail elsewhere[12] and, with the exception of the droplet train technique, only the important conclusions of these studies will be reviewed here.

The first indication of the enhanced reactivity of aqueous interfaces was observed in 1990 in the uptake of $SO_2$ by water droplets at a low pH.[12] The heterogeneous oxidation of $SO_2$ on aqueous aerosol in the atmosphere leads to the eventual production of sulfuric acid and acid rain. The enhanced reactivity of the aqueous interface was attributed to the rapid hydrolysis of the surface adsorbed $SO_2$ under strongly acidic and basic conditions to form a surface complex which then becomes fully solvated in the bulk phase.

$$SO_{2(ads)} + H_2O_{(aq)} \Leftrightarrow HSO_3^-H^+ \quad (9)$$

Uptake measurements were performed with a droplet train apparatus, probing the depletion of the trace gas concentration by mass spectroscopy or optical absorption.[12] This technique involves the production of a train of droplets of reproducible size, in the range 100–200 μm diameter, which flow through a trace gas under controlled conditions. The uptake of the trace gas by the aerosol droplets is probed by measuring the depletion of the trace gas concentration as the droplet surface area or exposure time (2–15 ms) of the droplets is varied.

More recent measurements have compared the pH dependent uptake of $CO_2$, $SO_2$ and $H_2S$, yielding a mass accommodation coefficient for $SO_2$ on water, and rate constants for the reactions of all three species with $OH^-$ on basic droplets. For the three systems, the reaction rate constants vary by 6 orders of magnitude, and support the view that the enhanced $SO_2$ uptake is due to a surface reaction pathway.[15]

Further support for the formation of a surface complex in the uptake of $SO_2$ was provided by surface tension and SHG measurements of the surface coverage of adsorbed $SO_2$ as a function of the bulk concentration.[17] In particular, a large decrease in surface tension with increase in aqueous S(IV) concentration was observed, an unusual trend for inorganic electrolyte solutions. It was recognised that other dissolved gases showing a similar trend can all readily be hydrolysed (HCl, $HNO_3$, $NH_4OH$, $NaHSO_3$ and $NaHCO_3$), further supporting the view that the surface complex was $HSO_3^-H^+$. The saturated surface coverage of the $SO_2$ complex was estimated as $5 \times 10^{14}$ molecules $cm^{-2}$.

The uptake of nitrogen oxides by aqueous droplets has also been extensively investigated. Recent droplet train measurements sought to verify an earlier investigation of the reactive surface uptake of $NO_2$ leading to the formation of nitric acid.[18] However, the upper limit placed on the reactive uptake coefficient ($\gamma < 5 \times 10^{-4}$) suggests that the chemistry occurring can be explained by bulk phase chemistry alone, failing to substantiate earlier measurements.

Droplet train measurements were used to examine the uptake of $N_2O_5$ on aqueous salt solutions at temperatures between 262 and 278 K.[19] On interaction with NaCl and NaBr solutions, $ClNO_2$ and $BrNO_2$ are formed. The uptake of $N_2O_5$ was observed to be independent of the identity and concentration of the salt, suggesting that the reaction products are formed by

reaction with the hydrolysis products of $N_2O_5$ uptake. This conclusion is also supported by earlier observations that the uptake of $N_2O_5$ on acidic solutions does not depend on the water content. Thus, the rate limiting step in the heterogeneous production of $ClNO_2$ and $BrNO_2$ is postulated to be the first step in the mechanism.

$$N_2O_{5(aq)} \Leftrightarrow NO_3^-{}_{(aq)} + NO_2^+{}_{(aq)} \quad (10)$$

$$NO_2^+{}_{(aq)} + X^- \rightarrow XNO_{2(aq)} \quad (11)$$

A more recent study has investigated the uptake of $N_2O_5$ on submicron sulfuric acid aerosol particles, with an acid composition in the range 26.3–64.5 wt%.[20] The uptake coefficient was observed to be independent of acid concentration, but showed a decrease with increase in temperature. The rate determining step was concluded to be the accommodation step, with reaction (10) providing the dominant pathway to $NO_2^+$ and thus $HNO_3$ at room temperature.

$$NO_2^+{}_{(aq)} + H_2O \rightarrow H^+ + HNO_{3(aq)} \quad (12)$$

The protonation of $N_2O_5$ was concluded to be the important pathway at low temperatures.

$$N_2O_{5(aq)} + H^+{}_{(aq)} \rightarrow HNO_{3\,(aq)} + NO_2^+{}_{(aq)} \quad (13)$$

The critical cluster size for mass accommodation was calculated to rise from 1.8 in 70 wt% sulfuric acid to 2.5 in 0 wt%.

The decomposition of HONO on submicron sulfuric acid aerosols proceeds by a surface reaction.[21] An Eley–Rideal mechanism is thought to be operative, with one gas phase molecule reacting with a HONO molecule already adsorbed at the liquid interface.

$$HONO_{\,(g)} + HONO_{\,(aq)} \rightarrow NO_{(g)} + NO_{2(g)} + H_2O_{(aq)} \quad (14)$$

When HONO is adsorbed by sulfuric acid aerosol particles in competition with HCl, a surface enhanced reaction at the liquid interface can occur, yielding ClNO and $H_2O$ as products.[22] This is similar to the acid catalysed reaction of HOCl and HCl on sulfuric acid aerosol particles.[23]

$$HOCl_{(aq)} + HCl_{(aq)} \rightarrow H_2O_{(aq)} + Cl_{2(g)} \quad (15)$$

The reaction rate constant was shown to increase with increasing acid concentration and it was concluded that the reaction may involve initially the protonation of HOCl, followed by the reaction of $H_2OCl^+$ with $Cl^-$. As HOCl adsorbs, competition between diffusion and reaction will determine the distribution within the liquid phase.

Studies of the uptake of HCl on aqueous sulfuric acid aerosols between 230 and 264 K and with acid concentrations between 39–69 wt% showed that the solubility of HCl decreases with increasing sulfuric acid concentration, preventing dissociation to solvated ions.[24] In contrast, the mass accommodation coefficient was shown to be independent of acid concentration, and inversely dependent on the temperature, suggesting that the HCl enters the liquid in the undissociated form and follows the critical cluster mechanism for phase transfer. More recent studies of the uptake of HCl, HBr and HI on aqueous surfaces between 262–281 K support the earlier conclusions.[25] With the uptake rate unchanged on basic droplets at pH 14 from that on neutral droplets, it was concluded that the uptake rate is determined by the solvation process at the interface and not by dissociation kinetics. The critical cluster sizes were calculated to be 2.1, 2.5 and 2.6 for HCl, HBr and HI, respectively, and follow the general trend of diminishing cluster size for molecules with increasing ability to hydrogen bond.

Isotope exchange studies have been used to probe the surface reactions of deuterated acetic acid, ethanol and water at the aqueous ($H_2O$) interface. For deuterated acetic acid and water, thermal accommodation at the interface is near unity, with all of the molecules colliding with the surface residing for sufficient time to undergo proton transfer.[26,27] At pH 7, the magnitude of the measured proton exchange probability for water cannot be explained by bulk phase like kinetics and must result from an enhanced surface reaction, probably involving the dangling OH bonds at the interface. When hydrogen bonding is possible with the gas phase molecule, adsorption is primarily through H-bonding with the dangling OH bonds. In contrast, the exchange probability for ethanol is 0.033 at 263 K and pH 7.[27] Ethanol exhibits both acid and base catalysed isotope exchange, with the exchange probability increasing at low and high pHs to values between 0.14–0.18. This can be understood from a kinetic model in which the ethanol can be adsorbed in two forms at the interface. In a weakly adsorbed state, proton transfer cannot occur. The ethanol must occupy a more partially solvated state closer to the bulk liquid before exchange is observed.

### 3.2 Probing the condensed phase

Uptake studies that probe the liquid phase directly are less extensive than those that probe the gas phase. The techniques available are more limited, although optical techniques have been used with some success, particularly in combination with single aerosol particle levitation techniques.[28]

The uptake dynamics of HCl by sulfuric acid aerosols were studied in single charged microdroplets, 30–70 μm in diameter, levitated in an electrostatic trap.[29] The changing size of the microdroplet over a period of up to 500 s was used to probe the uptake rate. Angle resolved elastic light scattering and electrostatic balancing of the increasing droplet mass were both used to determine the size change occurring. Two regimes in the uptake dynamics were observed. At low temperature and high sulfuric acid concentrations ($< 190$ K for 48 wt% acid and $< 195$ K for 56 wt% acid), liquid phase diffusion inside the droplet was observed to be rate limiting, permitting the calculation of the diffusion coefficients. At high temperatures and low sulfuric acid concentrations (185–207 K, 30–40 wt% acid), gas phase diffusion, accommodation and dissolution determined the uptake flux. A smooth transition between the two regimes was observed.

The sticking probabilities for the simultaneous binary condensation of nitric acid and water vapour on monodisperse condensation nuclei of diameter 80–150 nm were investigated by monitoring droplet growth rates from light scattering intensities at a fixed angle from a laser source.[10] Droplet radii grew to 0.5–4 μm, with the water partial pressure and nitric acid partial pressures being varied over as much as 3 orders of magnitude. The measurements permitted the mass and thermal accommodation coefficients to be isolated and determined. Assuming that the value of $\alpha$ for water accommodated on a water surface is unity and the thermal accommodation coefficient for both water and nitric acid is unity, $\alpha$ was calculated to be between 0.3 and 1 for nitric acid on a water surface.

Direct measurements of changing composition on large droplets, 2–3 mm in diameter, have been made by absorption spectroscopy over a period of up to 400 s.[30] The size of the droplets enables such *in situ* measurements to be made. The uptake dynamics of $HNO_3$ and $N_2O_5$ on pure water and $O_3$ on NaI solutions were examined by recording the time dependent absorption spectra in the wavelength range 240–800 nm. The values of $\alpha$ were calculated to be $> 3 \times 10^{-2}$, $1.1 \times 10^{-2}$ and $> 2 \times 10^{-2}$, respectively.

### 3.3 Probing the interfacial region

The scattering of molecules from liquid surfaces with low vapour pressure has yielded many important insights into the dynamics occurring in the interfacial region.[11] Unlike the

uptake experiments described in the preceding sections, the gas molecules do not possess a thermally averaged distribution of kinetic energies, but a well defined kinetic energy, produced in a molecular beam directed at the liquid surface. In addition, the studies must be performed on liquids of low vapour pressure, such as long-chain hydrocarbons, glycerol and concentrated sulfuric acid. This prevents collisions between gas phase molecules above the surface obscuring the interfacial dynamics. Thus, the molecular beam technique provides complementary information to that obtained by the studies of thermally averaged uptake on high vapour pressure liquids already discussed. Gases that have been investigated include inert atomic gases (such as Ar and Xe), simple hydrocarbon molecules (such as methane and propene), and protic gases (such as water, ammonia, alcohols and carboxylic acids).

By examining the kinetic energy distribution of the gas molecules scattered from the surface, fundamental questions about the nature of the interactions between the gas molecules and the interface, and the mechanism of mass accommodation have been addressed. The molecules scattered from the surface exhibit two types of scattering behaviour: inelastic scattering and trapping desorption. The former results in impulsive energy transfer with the surface but no further outcome. The latter, also referred to as thermal accommodation, results from multiple collisions with the surface and transient residency at the interface before desorption.

The nature of attractive forces encountered at the liquid interface by impinging gas phase molecules has been investigated by comparing the inelastic scattering and trapping desorption of Ne, $CH_4$, $NH_3$ and $D_2O$ from both a hydrocarbon surface, squalane, and a hydrogen bonding surface, glycerol.[11] The fraction of molecules undergoing trapping desorption from the glycerol surface compared to inelastic scattering increases with the ability of the scattering molecule to hydrogen bond (*i.e.* Ne < $CH_4$ < $NH_3$ and $D_2O$). Conversely, the fraction of collisions that lead to thermal desorption is larger for Ne and $CH_4$ from the squalane surface than from the glycerol.

Molecular beam techniques have been used to examine the interaction of HCl, HBr and $HNO_3$ with a liquid sulfuric acid surface at 213 K to investigate the fate of the HX molecule after thermalisation at the $D_2O/D_2SO_4$ surface.[31] All three molecules temporarily become trapped at the surface, but only a small fraction of the thermally desorbed HCl and HBr (11% and 22%, respectively) undergo deuterium exchange, consistent with the droplet train techniques which conclude that HCl is accommodated on acidic droplets without dissociation. The residence times of HCl and HBr molecules that are thermally desorbed are estimated to be less than 2 μs. The HCl, HBr and $HNO_3$ that undergo reaction have residency times of 50 μs, 3 ms and 0.1 s, respectively, implying that desorption of thermalised HCl and HBr is more rapid than solvation and reaction. In contrast, 95% of $HNO_3$ undergoes deuterium exchange, and this may be due to stronger hydrogen bonding with the interface.

The interaction of HCl, DCl and HBr with a liquid glycerol surface has also been explored.[32] SFG studies of the glycerol surface have indicated that all surface OH groups are hydrogen bonded, with the carbon skeleton lying approximately perpendicular to the surface plane. The molecular beam studies showed that the thermal accommodation of HCl and HBr occurs easily with dissipation of excess kinetic energy as large as 100 kJ $mol^{-1}$. This is consistent with droplet train measurements for the uptake of DCl on ethylene glycol, which showed that the thermal accommodation coefficient was near 1.[33] The lifetime of thermally accommodated HBr molecules is longer than 10 s. In contrast, 20% of HCl desorbs rapidly before dissociation, while the HCl that dissolves reversibly with dissociation has a lifetime between 0.1–2 s at the surface. This is again consistent with the droplet train studies of the uptake of HBr on ethylene glycol droplets which showed that HBr interacts more strongly than HCl with hydrophilic surfaces.[33]

## 4 The chemistry of ammonia on aqueous droplets

Ammonia is the dominant soluble basic gas in the atmosphere (0.1–10 ppb) and is responsible for neutralising acidic aerosols. This process commonly leads to the production of non-volatile ionic salts within the condensed phase. Gas-phase reactions of ammonia are slow and therefore aerosols provide a substantial sink for tropospheric ammonia. However, the maximum concentration of ammonia observed in aerosols is only equal to the concentration of the neutralising acidic species within the aerosol droplet.[3] From this observation it has been concluded that, following adsorption of ammonia and neutralisation of the droplet to pH 7, any excess ammonia is adsorbed on the droplet surface forming a complex with water. This surface complex inhibits any further uptake of ammonia from the gas phase.

SFG studies have probed the orientation of ammonia at the aqueous interface and the nature of the water–ammonia surface complex.[3,8] The symmetric stretching vibration of ammonia is only slightly red-shifted from the gas phase vibrational frequency, suggesting that the adsorption leads to little perturbation of the N–H bonding. At low coverages of ammonia, the SFG spectra imply that the availability of the free/dangling OH bonds diminishes as ammonia forms hydrogen-bonds at the surface; the lone pair on the nitrogen interacts with the dangling bond. Ab initio calculations predict that the O–H···N hydrogen bond configuration is virtually linear. This conclusion is supported by the SFG studies which suggest that the ammonia is tilted on average between 25° to 38° to the surface normal and that free rotation about the $C_3$ axis of the adsorbed ammonia molecule remains possible.

The temperature dependence of the surface tension of aqueous ammonia solutions has been used to explore the existence of the ammonia–water surface complex, yielding a value for $\Delta G_{ads}$ of $-19.1 \pm 0.5$ kJ $mol^{-1}$.[34] A saturated surface coverage of $(1.2 \pm 0.2) \times 10^{14}$ molecule $cm^{-2}$ was calculated, which is close to the estimated surface density of free O–H groups reported by Shen of $2 \times 10^{14}$ molecule $cm^{-2}$.[5] Ab initio calculations suggested that the most important features of the surface bound state are captured by an ammonia molecule bound simultaneously to two surface water molecules, accounting for the $\Delta H_{ads}$ experimentally determined. The critical cluster size is predicted to be between 2–3 water molecules.

Recent droplet train measurements have probed the uptake of ammonia on aqueous surfaces as a function of pH (0–13) and temperature.[35,36] At low pHs, the uptake is limited by the mass accommodation process, and $\gamma \sim \alpha$. The mass accommodation coefficient was found to decrease with increase in temperature, providing a picture of ammonia uptake that is consistent with the critical cluster model. At high pH, the uptake is governed by the bulk phase solubility of ammonia and surface processes. On the timescale of the experiments, a surface complex (probably $NH_4^+$–$OH^-$) rapidly reaches a steady state at the interface in equilibrium with the gas-phase, giving a one off uptake of ammonia that is achieved under the experimental conditions on a very short timescale. The uptake coefficient is time dependent reflecting the changing dependence of the bulk phase solubility as the ammonia is accommodated and the Henry's law saturation is approached. The calculated surface coverage of the complex is estimated to be considerably larger than surface excess calculated from surface tension data. This also suggests that the ammonia species resident at the surface must be present as a complex that is stable and resists transport into the droplet bulk.

The uptake of ammonia on sulfuric acid solutions over the temperature range 248–288 K and composition range 20–70 wt% sulfuric acid has also been studied. Reaction of accommodated ammonia with $H^+$ at the gas liquid interface leading to the production of $NH_4^+$, is responsible for the enhanced uptake coefficient at high acid concentrations, with the uptake coefficient reaching 1 at 55 wt% sulfuric acid.[36]

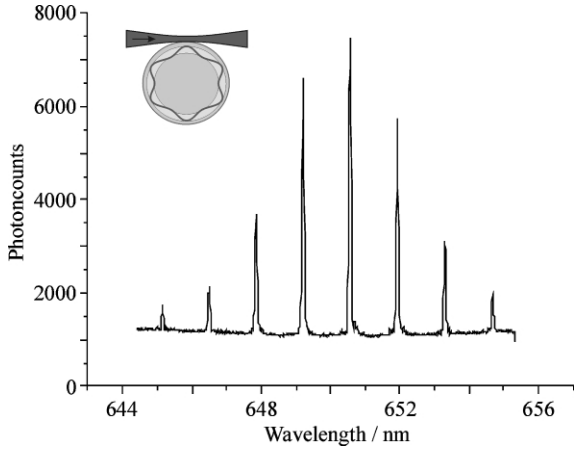


**Fig. 5** A cavity enhanced Raman signature of a single droplet achieved with a single laser shot at 532 nm, by aligning the laser beam to the edge of the droplet as shown. The Raman signature occurs within the water Raman band and the progression of peaks can be used to determine the radius of the droplet with a precision of ± 1 nm.

We are currently developing methods to use laser techniques to probe the changing size and composition of single water droplets directly, with initial studies focusing on the uptake of ammonia on acidic water droplets.[37,38] The changing size and composition of a liquid droplet can be monitored by cavity enhanced Raman scattering.[39,40] A laser pulse illuminates a single liquid droplet with the illumination geometry shown in Fig. 5. At this geometry, the laser light may become trapped within a cavity resonance, with the light undergoing total internal reflection many times within the droplet at the liquid–air interface. The light may circulate for timescales of the order of nanoseconds, with Raman scattering of the light by the droplet constituents. Raman scattering is stimulated at Raman scattered wavelengths that are also trapped within cavity resonances, yielding a spectral fingerprint which is characteristic of the droplet size.

We are also applying a laser induced fluorescence technique combined with a droplet train apparatus, which can probe the pH of water droplets directly.[37] By seeding the water droplets with an appropriate dye and, following a well-characterised exposure time to ammonia gas, exciting the dye molecule with a pulsed laser, the pH of the droplet can be readily determined from the dispersed fluorescence spectrum. The dye molecule, D, and the protonated form, $DH^+$, fluoresce at different wavelengths. By measuring the intensity of the fluorescence at two wavelengths, the ratio $D/DH^+$, and hence droplet pH, can be calculated from a simple calibration curve. The variation in the fluorescence spectrum and the corresponding calibration curve are illustrated in Fig. 6. Preliminary studies have indicated that this technique can be used to probe the changing pH of water droplets directly as the droplets adsorb ammonia, complementing existing experiments. Combining the fluorescence technique with cavity enhanced spectroscopy could enable spatially resolved measurements of droplet pH to be made.

## 5 Summary

An improved understanding of heterogeneous atmospheric aerosol chemistry is dependent on a close collaboration between laboratory experiments, field measurements of aerosol particle composition and size, theoretical simulation of interfacial dynamics and atmospheric modelling. At present, there is a substantial gap between what can be studied experimentally under controlled laboratory conditions and the complexity of atmospheric aerosol systems revealed by field measurements. Attempts must be made to bridge this gap by using laboratory techniques to examine the dynamics of multicomponent and

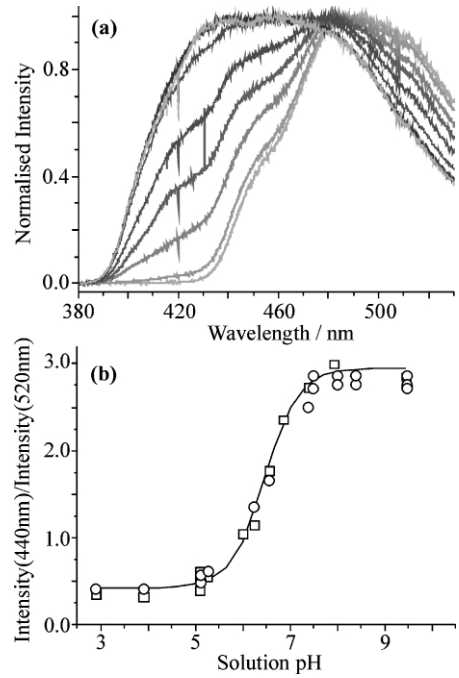


**Fig. 6** (a) The change in fluorescence spectrum for droplets of pH 10.5, 7.6, 6.9, 6.6, 6.4, 5.7, 4.8, 1.4 (with increase in peak fluorescence wavelength for decreasing droplet pH). (b) A calibration curve can be calculated from the fluorescence spectra, providing a direct way of monitoring the uptake of an acidic or basic reagent from the gas phase by a liquid droplet (squares – bulk phase calibration, circles – droplet).

multiphase aerosols under conditions relevant to the atmosphere. Over recent years, laboratory measurements have enabled general fundamental factors governing heterogeneous chemistry to be elucidated. The correlation between $\Delta H_{obs}$ and $\Delta S_{obs}$ for the uptake of a range of non-reactive trace species on water droplets, as identified by Davidovits *et al.*,[13] is central to our understanding of accommodation at the liquid interface through the formation of a critical cluster. A full theoretical treatment of the uptake process, which not only examines the thermodynamics for accommodation but also the kinetics, is yet to be developed.[14] From the complementary information gained through droplet trains studies, in which the gas phase composition is probed, molecular beam studies of the interface, and techniques that probe the condensed phase, a more refined understanding of reactive uptake is evolving. The challenge is now to enhance the partnership of laboratory measurements with field studies to improve our understanding of heterogeneous atmospheric aerosol chemistry.

## 6 Acknowledgements

RMS acknowledges the support of the EPSRC ATAC program for postdoctoral support.

## 7 References

1 J. H. Seinfeld and S. N. Pandis, *Atmospheric Chemistry and Physics: From Air Pollution to Climate Change*, John Wiley & Sons, 1998.
2 A. W. Adamson and A. P. Gast, *Physical Chemistry of Surfaces*, John Wiley & Sons, Inc., 1997.
3 M. J. Shultz, S. Baldelli, C. Schnitzer and D. Simonelli, *J. Phys. Chem. B*, 2002, **106**, 5313.
4 M. C. Goh, J. M. Hicks, K. Kemnitz, G. R. Pinto, K. Bhattacharyya, K. B. Eisenthal and T. F. E. Heinz, *J. Phys. Chem.*, 1988, **92**, 5074.
5 Q. Du, R. Superfine, E. Freysz and Y. R. Shen, *Phys. Rev. Lett.*, 1993, **70**, 2313.

6 E. Demou and D. J. Donaldson, *J. Phys. Chem. A*, 2002, **106**, 982.
7 D. J. Donaldson and D. Anderson, *J. Phys. Chem. A*, 1999, **103**, 871.
8 D. Simonelli and M. J. Shultz, *J. Chem. Phys*., 2000, **112**, 6804.
9 C. Schnitzer, S. Baldelli, D. J. Campbell and M. J. Shultz, *J. Phys. Chem. A*, 1999, **103**, 6383.
10 R. Rudolf, A. Vrtala, M. Kulmala, T. Vesala, Y. Viisanen and P. E. Wagner, *J. Aerosol Sci*., 2001, **32**, 913.
11 G. M. Nathanson, P. Davidovits, D. R. Worsnop and C. E. Kolb, *J. Phys. Chem*., 1996, **100**, 13007.
12 C. E. Kolb,, D. R. Worsnopp, M. S. Zahniser, P. Davidovits, , L. F. Keyser, , M.-T. Leu, , M. J. Molina, , D. R. Hanson and , and A. R. Ravishankara, *Laboratory studies of atmospheric heterogeneous chemistry*, in *Progress and problems in atmospheric chemistry*, ed. J. R. Barker, Singapore, 1995.
13 P. Davidovits, J. H. Hu, D. R. Worsnop, M. S. Zahniser and C. E. Kolb, *Faraday Discuss*., 1995, **100**, 65.
14 T. Somasundaram, R. M. Lynden-Bell and C. H. Patterson, *Phys. Chem. Chem. Phys*., 1999, **1**, 143.
15 J. Boniface, Q. Shi, Y. Q. Li, J. L. Cheung, O. V. Rattigan, P. Davidovits, D. R. Worsnop, J. T. Jayne and C. E. Kolb, *J. Phys. Chem. A*, 2000, **104**, 7502.
16 D. R. Hanson, *J. Phys. Chem.B*, 1997, **101**, 4998.
17 D. J. Donaldson, J. A. Guest and M. C. Goh, *J. Phys. Chem*., 1995, **99**, 9313.
18 J. L. Cheung, Y. Q. Li, J. Boniface, Q. Shi, P. Davidovits, D. R. Worsnop, J. T. Jayne and C. E. Kolb, *J. Phys. Chem. A*, 2000, **104**, 2655.
19 F. Schweitzer, P. Mirabel and C. George, *J. Phys. Chem. A*, 1998, **102**, 3942.
20 M. Hallquist, D. J. Stewart, J. Baker and R. A. Cox, *J. Phys. Chem. A*, 2000, **104**, 3984.
21 J. Baker, S. F. M. Ashbourn and R. A. Cox, *Phys. Chem. Chem. Phys*., 1999, **1**, 683.
22 C. A. Longfellow, T. Imamura, A. R. Ravishankara and D. R. Hanson, *J. Phys. Chem. A*, 1998, **102**, 3323.
23 D. J. Donaldson, A. R. Ravishankara and D. R. Hanson, *J. Phys. Chem. A*, 1997, **101**, 4717.
24 G. N. Robinson, D. R. Worsnop, J. T. Jayne, C. E. Kolb, E. Swartz and P. Davidovits, *J. Geophys. Res*., 1998, **103**, 25371.
25 F. Schweitzer, P. Mirabel and C. George, *J. Phys. Chem. A*, 2000, **104**, 72.
26 Y. Q. Li, P. Davidovits, Q. Shi, J. T. Jayne, C. E. Kolb and D. R. Worsnop, *J. Phys. Chem. A*, 2001, **105**, 10627.
27 Q. Shi, Y. Q. Li, P. Davidovits, J. T. Jayne, D. R. Worsnop, M. Mozurkewich and C. E. Kolb, *J. Phys. Chem. B*, 1999, **103**, 2417.
28 E. J. Davis, *Aerosol Sci. Technol*., 1997, **26**, 212.
29 M. Schwell, H. Baumgartel, I. Weidinger, B. Kramer, H. Vortisch, L. Woste, T. Leisner and E. Ruhl, *J. Phys. Chem. A*, 2000, **104**, 6726.
30 M. Schutze and H. Herrmann, *Phys. Chem. Chem. Phys*., 2002, **4**, 60.
31 J. R. Morris, P. Behr, M. D. Antman, B. R. Ringeisen, J. Splan and G. M. Nathanson, *J. Phys. Chem. A*, 2000, **104**, 6738.
32 B. R. Ringeisen, A. H. Muenter and G. M. Nathanson, *J. Phys. Chem. B*, 2002, **106**, 4988.
33 Y. Q. Li, H. Z. Zhang, P. Davidovits, J. T. Jayne, C. E. Kolb and D. R. Worsnop, *J. Phys. Chem. A*, 2002, **106**, 1220.
34 D. J. Donaldson, *J. Phys. Chem. A*, 1999, **103**, 62.
35 Q. Shi, P. Davidovits, J. T. Jayne, D. R. Worsnop and C. E. Kolb, *J. Phys. Chem. A*, 1999, **103**, 8812.
36 E. Swartz, Q. Shi, P. Davidovits, J. T. Jayne, D. R. Worsnop and C. E. Kolb, *J. Phys. Chem. A*, 1999, **103**, 8824.
37 R. Gatherer and J. P. Reid, *Chem. Phys. Lett*., 2002, **357**, 153.
38 R. D. B. Gatherer, R. M. Sayer and J. P. Reid, *Chem. Phys. Lett*., 2002, **366**, 34.
39 H. B. Lin and A. J. Campillo, *Opt. Lett*., 1995, **20**, 1589.
40 H. M. Tzeng, K. F. Wall, M. B. Long and R. K. Chang, *Opt. Lett*., 1984, **9**, 273.